Negative refraction and tiling billiards

Diana Davis, Kelsey DiPietro, Jenny Rustad, Alexander St Laurent

June 12, 2015

Abstract

We introduce a new dynamical system that we call *tiling billiards*, where trajectories refract through planar tilings. This system is motivated by a recent discovery of physical substances with negative indices of refraction. We investigate several special cases where the planar tiling is created by dividing the plane by lines, and we describe the results of computer experiments.

1 Introduction

1.1 Negative index of refraction in physics

When light travels from one medium to another, the path of the light may bend; this bending is known as *refraction*. Snell's Law[1] describes the change in angle of the path, relating it to the indices of refraction of the two media. If θ_1 and θ_2 are the angles between the ray and the normal to the boundary in each medium, and k_1 and k_2 are the indices of refraction of the two media,

$$\frac{\sin\theta_1}{\sin\theta_2} = \frac{k_2}{k_1}.$$

This ratio is called the *refraction coefficient* or the *Snell index*.

In nature, the indices of refraction of all materials are positive, and negative refraction was once a theoretical fantasy. Recently, however, physicists have created media that have negative indices of refraction, called "metamaterials." Articles describing this discovery were published in *Science*, and have been cited thousands of times in the 10 years since [13], [12].

Even with standard materials with positive indices of refraction, it is possible to do counterintuitive things like make glass "disappear" by immersing it in clear oil. Since metamaterials are not found in nature, we have even less intuition for their effects. When light crosses a boundary between a medium with a positive index of refraction and one with a negative index of refraction, the light bends in the opposite direction as it would if both media had positive indices of refraction. These new materials may someday be used to create an invisibility shield, improve solar panel technology, or fabricate a perfect lens that would be able to resolve details even smaller than the wavelengths of light used to create the image [16].

The behavior in complex scenarios, such as the propagation of light through materials that alternate between standard materials and metamaterials, is complex and interesting. That is the type of system that we study in this paper, and it introduces a new dynamical system, motivated by this discovery in physics.

1.2 The tiling billiards mathematical model

We consider a model for light passing between two media with refraction coefficient -1, so that the light is "reflected" across the boundary. Our dynamical system is as follows:

[1] Willebrord Snell stated this result in 1621, but it was known in 984 to Islamic scholar Abu Said al-Ala Ibn Sahl [5].

1. We consider a partition of the plane into regions (a *tiling*).

2. We give a reflection rule for a beam of light passing through the tiling: When light hits a boundary, it is reflected across the boundary.

To relate this model to the physical system with standard materials and metamaterials, we consider a two-colorable tilling of the plane, where one color corresponds to a material with index of refraction k, and the other color to a material with index $-k$. However, the dynamical system described above need not obey this restriction.

Note that this problem is 1-dimensional, in the sense that the width of a parallel beam of light is preserved.

In this paper, we study the case where the plane is divided by lines into regions (possibly of infinite area). Such a tiling is always two-colorable, because finitely many lines intersect at any point, and every vertex has an even valence, so the associated adjacency graph of the regions contains no odd cycles, and is thus bipartite. Within this case, we study the three special cases where the plane is divided by a finite number of lines, where the resulting tiling is of congruent triangles with 6 meeting at each vertex, and where the resulting tiling is of alternating regular hexagons and triangles (the *trihexagonal* tiling).

1.3 Parallels with inner and outer billiards

The tiling billiards system is new, but it has many similarities to the well-studied dynamical systems of inner and outer billiards. In the *inner billiards* dynamical system, we consider a billiard table with a ball bouncing around inside, where the angle of incidence equals the angle of reflection at each bounce. In the *outer billiards* dynamical system, the ball is outside the table, and reflects along a tangent line to the table (or through a vertex of a polygonal table), so that the original distance from the ball to the reflection point is equal to the distance from the reflection point to the image [14]. In tiling billiards, the ray is reflected across the boundary. Examples of inner, outer and tiling billiards are in Figure 1.

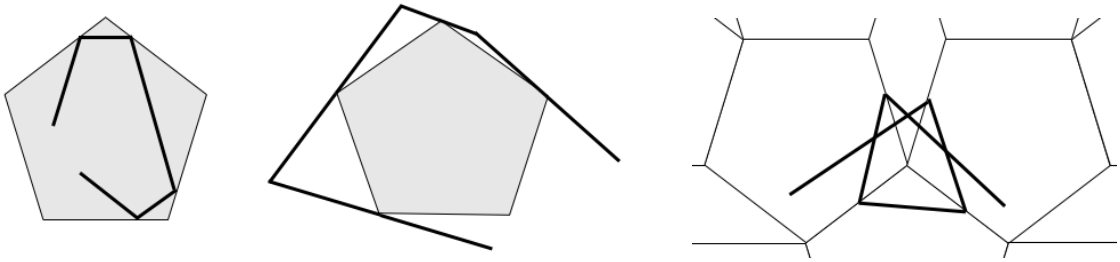

Figure 1: Part of (a) an inner billiards trajectory on a regular pentagon, (b) an outer billiards trajectory on a regular pentagon, (c) a tiling billiards trajectory on a planar tiling of pentagons and rhombi

Tiling billiards is a cross between the two systems, in the sense that in inner billiards, the ray is reflected across the normal to the boundary; in outer billiards, the ray itself forms a tangent to the boundary and is reflected through the point of tangency; and in tiling billiards, the light ray is reflected across the tangent to the boundary (or the boundary itself if it is polygonal).

Much of the literature on billiards is for polygonal billiards. For this system, the analogue is a polygonal tiling of the plane, which we study here.

For any billiard system, there are several basic questions to ask. We outline these below, and compare results from the established literature on inner and outer billiards to our observations and results about tiling billiards in the special cases that we investigated.

Are there periodic trajectories?

In inner billiards on a rational polygon (a polygonal table where every angle is a rational multiple of π), there are always periodic paths – in fact, Masur showed that periodic directions are dense [7]. For general polygons, it is not known whether there is always a periodic path, but Schwartz showed that for in inner billiards on a *triangle* whose largest angle is less than 100°, there is always a periodic trajectory [9]. In outer billiards on a polygon whose vertices are at lattice points, all of the orbits are periodic [15], [10].

We study several special cases of the tiling billiards system, and find periodic trajectories in every one. Every triangle tiling has a periodic trajectory of period 6 around a vertex (Corollary 3.2), and almost all have a period-10 trajectory around 2 vertices (Theorem 3.11).

Can trajectories escape?

After the outer billiards system was introduced by B.H. Neumann, it stood as an open question for decades whether there are billiard tables with unbounded orbits, with many negative answers for special cases. Finally, Schwartz discovered that the Penrose kite has unbounded orbits [11], and Dolgopyat and Fayad discovered the same for the half disk [2].

We show that every right triangle tiling has an unbounded trajectory (Theorem 3.7). In tiling billiards on tilings with translational symmetry, we frequently have a type of very regular escaping trajectory, which we call a *drift-periodic* trajectory: it is not periodic, but is periodic up to translation, like a staircase. We show that some right triangle tilings have drift-periodic trajectories (Theorem 3.9), and based on computer experiments we conjecture that they all do. We prove the existence of several families of drift-periodic trajectories on the trihexagonal tiling, and based on computer experiments we conjecture that there are non-periodic escaping trajectories as well. We also study a division of the plane by finitely many lines, all of which trivially have escaping trajectories that reflect only once, and some of which have trajectories that escape by spiraling outward.

Can a trajectory fill a region densely?

In inner billiards on a square table, a trajectory with an irrational slope is dense. It is also possible to construct a table so that some trajectory on that table is dense in one part of the table, but never visits another part of the table at all [8].

We construct several families of drift-periodic trajectories in the trihexagonal tiling, the limiting members of which fill regions of the tiling densely (Corollary 4.11).

Is the behavior stable under small perturbations of the starting point and direction of the trajectory, and under small perturbations of the billiard table?

In inner billiards on a square table, the behavior of the trajectory depends on the direction: directions with rational slope yield periodic trajectories, and with irrational slope yield dense trajectories, so a small perturbation changes everything. Similarly, a small perturbation of the polygon taking the square to a nearby quadrilateral with different angles yields very different behavior of the trajectory. So inner billiards can be highly sensitive to the starting conditions, and in this sense are not stable. In contrast, outer billiards are quite stable: if one point yields a periodic trajectory, that point lies in a polygonal region of points that all do the same thing.

The most surprising observation that we made relates to this question: As mentioned above, we found that the trihexagonal tiling exhibits very unstable behavior: a slight perturbation of the direction wildly changes the trajectory. For example, in trying to find periodic trajectories with our computer program, we had to be extremely precise with the mouse and a tiny change would lead to a trajectory that escaped to infinity.[2] In contrast, triangle tilings have extremely stable behavior; changing the direction, or starting location, or angles and lengths of the tiling triangle, only superficially changes the trajectory. For example, at one point we conjectured that some behavior does not depend on the starting position, because even a vast difference in moving the mouse had an imperceptible effect on the trajectory. We had trouble proving it, and found that when we "zoomed in" many times in our program, the starting conditions did actually have a tiny effect. In this sense,

[2] A version of our program is available online at `http://awstlaur.github.io/negsnel/`.

triangle tilings are similar to outer billiards in their stability, and the trihexagonal tiling is similar to inner billiards in its instability.

Is the behavior invariant under affine transformations?

Because the outer billiards system uses lengths, it is invariant under affine transformations; the dynamics on any parallelogram are the same as the dynamics on a square, and the dynamics on every triangle are the same. Because the inner billiards system uses angles, it is highly sensitive to such changes; inner billiards on a rectangular table is equivalent to that of a square table, but inner billiards on a general parallelogram is completely different.

The tiling billiards system shares all of these characteristics with the inner billiards system, because it also uses angles. For example, every right triangle tiling has an escaping trajectory (Theorem 3.7), but the equilateral triangle tiling has only periodic trajectories of period 6 around the vertices, and no escaping trajectories (Theorem 1.1).

In this paper, we address the question of periodic and drift-periodic trajectories in each of the three types of tilings we studied. We have results on periodic, escaping and dense trajectories. While we have observations and conjectures about the stability of trajectories on various tilings, and other basic questions about this dynamical system, exploration of the system remains almost completely open.

1.4 Previous results on tiling billiards

Mascarenhas and Fluegel asserted in [6] that every trajectory in the equilateral triangle tiling, and in the $30°$-$60°$-$90°$ triangle tiling, is periodic, and that every trajectory in the square tiling is either periodic or drift-periodic. All of these tilings, and example trajectories, are in Figure 2.

In [3], Engelman and Kimball proved that there is always a periodic trajectory about the intersection of three lines (see Figure 4), and there is no periodic orbit about the intersection of two non-perpendicular lines. In Section 2, we generalize these results to certain divisions of the plane by any finite number of lines.

Because neither [6] nor [3] is in the published literature, we include these results and their proofs here, for completeness. We also add the regular hexagon tiling, so that we have all three tilings by regular polygons (even though the hexagon tiling is not two-colorable).

Theorem 1.1 (Mascarenhas and Fluegel)**.** *Every trajectory is periodic in the equilateral triangle tiling and in the* $30°$-$60°$-$90°$ *triangle tiling triangle tiling. Every trajectory in the square tiling and in the regular hexagon tiling is either periodic or drift-periodic.*

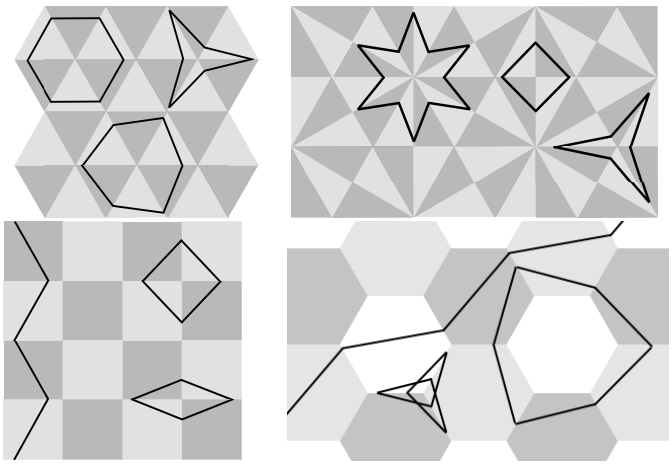

Figure 2: Trajectories in these four basic tilings have very simple dynamics

Proof. Each of these tilings is reflection-symmetric across every line of the tiling. (Note that there are many tilings of $30°$-$60°$-$90°$ triangles; Mascarenhas and Fluegel chose the one pictured in Figure 2b.) Thus, every trajectory that crosses a given line is also reflection-symmetric across that line. In the triangle tilings, a trajectory going from one edge of a triangle to another always crosses an adjacent edge, so under the reflectional symmetry it closes up into a periodic path with the valence of the vertex, which is always 6 in the equilateral triangle tiling, and is 4, 6 or 12 in the $30°$-$60°$-$90°$ triangle tiling tiling (Figure 2 (a) and (b)).

In the square tiling, a trajectory that starts on one edge either crosses the adjacent edge or the opposite edge. If it crosses the adjacent edge, it circles around the vertex between those edges, so it closes up into a periodic path with the valence of the vertex: 4. If it crosses the opposite edge, it "zig-zags" in a drift-periodic path of period 2 (Figure 2 (c)). Similarly, in the regular hexagon tiling, a trajectory crosses the adjacent edge, the next-to-adjacent edge, or the opposite edge. If it crosses the adjacent edge or next-to-adjacent edge, it closes up into a periodic path of period 6, and if it crosses the opposite edge, it zig-zags as in the square tiling (Figure 2 (d)). □

To extend the comparison with inner and outer billiards systems, we give an alternative proof of this result. In inner billiards, a common technique is to "unfold" the trajectory across the edges of the table, creating a new copy of the table in which the trajectory goes straight. Analogously but going the opposite direction, in tiling billiards we can "fold up" the tiling so that congruent tiles are on top of each other, and the trajectory goes back and forth as a line segment between edges of a single tile (Figure 3).

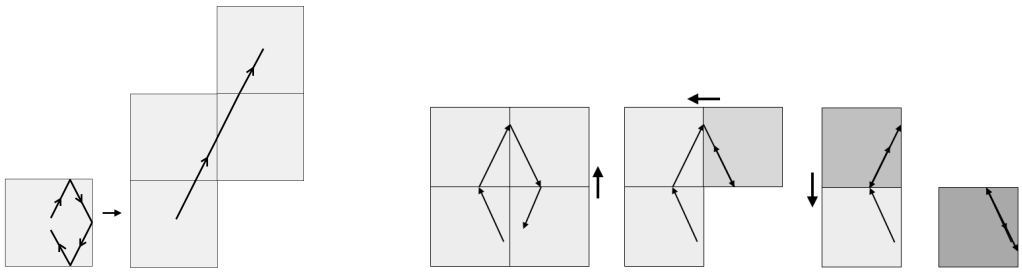

Figure 3: (a) Unfolding a trajectory on the square billiard table into a straight line (b) Folding a trajectory on the square tiling into a segment

Alternative proof of Theorem 1.1 using folding. Each of the four tilings is reflection-symmetric across every edge of the tiling, so when a trajectory crosses an edge from one tile to another, that edge is a line of symmetry for the two adjacent tiles, and we fold one tile onto the other. When we fold up a trajectory this way, it is a line segment going back and forth between two edges of the tile, so every trajectory is periodic or drift-periodic. For a periodic trajectory, the period is the number of copies needed for the trajectory to return to the same edge in the same place, which for a vertex of valence v is v when v is even and $2v$ when v is odd. For a drift-periodic trajectory, the period is the number of copies needed for the trajectory to return to a corresponding edge in the same place, which in both the square and hexagon tiling is 2. □

Theorem 1.2 (Engelman and Kimball)**.** *(a) There is a periodic trajectory about the intersection of two lines if and only if the lines are perpendicular. (b) There is always a periodic trajectory about the intersection of three lines.*

Proof. (a) Suppose that the two lines intersect at an angle α, and the initial angle between the trajectory and a line is θ, measured on the same side as α. If a trajectory is periodic, then it must be $4k$-periodic for some natural number k, since it must cross both lines twice to return to its starting trajectory. If the initial angle is θ, the first four angles between the trajectory and the lines are $\theta, \alpha - \theta, \pi + \theta - 2\alpha, 3\alpha - \pi - \theta$, and then $\theta + 4\alpha - 2\pi$ with the original line. By induction, we see that the k^{th} time the trajectory returns to the original line, it will make the angle $\theta + k(4\alpha - 2\pi)$. For

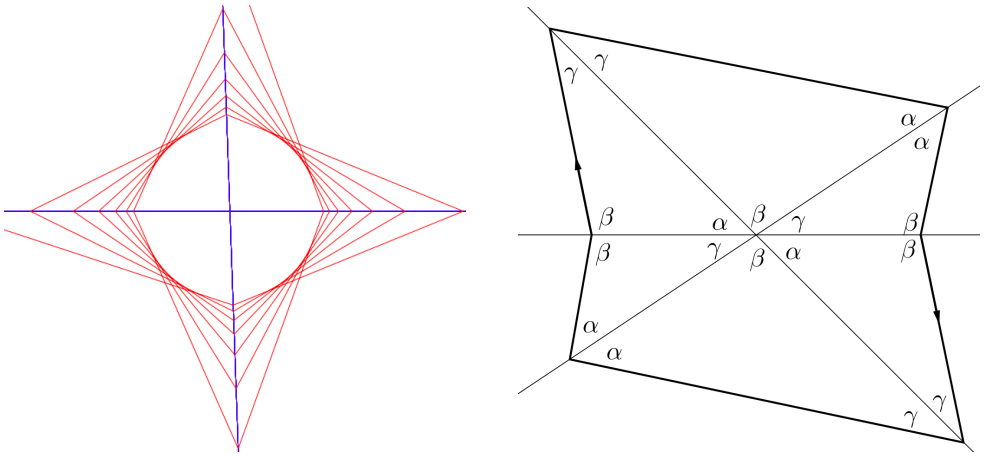

Figure 4: (a) There is no periodic trajectory about two non-perpendicular lines
(b) There is always a periodic trajectory about the intersection of three lines

the trajectory to be periodic, we need this to be equal to the initial angle, so in a $4k$-periodic orbit, $\theta + k(4\alpha - 2\pi) = \theta$, which occurs if and only if $\alpha = \pi/2$. The lengths are then trivially equal, so the trajectory is periodic, and must have period 4.

An example of the non-perpendicular behavior is given in Figure 4 (a), where the lines meet at $88°$.

(b) Label the angles of intersection between the three lines α, β and γ, so $\alpha + \beta + \gamma = \pi$. If we start a trajectory on the line between angles α and γ with initial angle β (Figure 4 (b)), then when the trajectory returns to the same line, by symmetry it will have the same angle. It will also be at the same point; the length is calculated via a simple Law of Sines argument. Then the trajectory is periodic with period 6. □

Glendinning studies a system that is similar to ours: a "chessboard" tiling where the two colors of tiles have different positive indices of refraction, in particular where the refraction coefficient is greater than 1. This is similar to our setup, except that the angle at a boundary changes, which leads to different behavior than in our system. He finds that the number of angles with which any ray intersects the square lattice is bounded, and that if the refraction coefficient is high enough, one can use interval exchange transformations to describe the dynamics.

1.5 Results presented in this paper

First, we prove general results about several classes of triangle tilings by congruent triangles.

Definition 1.3. We say that a *triangle tiling* is a tiling by congruent triangles that meet 6 at a vertex with half-turn symmetry around every vertex, or equivalently a grid of parallelograms with parallel diagonals.

We call a trajectory *periodic* if it repeats. We call a trajectory *drift-periodic* if there exist infinitely many distinct congruent tiles, where the trajectory crosses corresponding edges in the same place, at the same angle, and consecutive corresponding points differ by a constant vector.

The *trihexagonal tiling* has a regular hexagon and an equilateral triangle meeting at every edge.

First, we divide the plane by a finite number of non-parallel lines n.

Theorem 2.6: For $n \geq 3$ odd, there is always a periodic trajectory.

Theorem 2.10: For $n \geq 2$ even, there is a periodic trajectory if and only if the counter-clockwise angles $\alpha_0, \ldots, \alpha_{n-1}$, between consecutive lines ordered by angle, satisfy

$$0 = \alpha_0 - \alpha_1 + \alpha_2 - \alpha_3 + \cdots + \alpha_{n-4} - \alpha_{n-3} + \alpha_{n-2} - \alpha_{n-1}.$$

Next, we study triangle tilings.

Theorem 3.4: In an isosceles triangle tiling, all orbits are either periodic or drift-periodic.

Theorem 3.7: Every right triangle tiling has an escaping trajectory.

We prove this by construction: if a trajectory bisects a hypotenuse, then it is unbounded.

Theorem 3.9: If the smallest angle of a right triangle tiling is $\frac{\pi}{2n}$ for some $n \in \mathbb{N}$, then a drift-periodic orbit exists.

Theorem 3.11: Every triangle tiling, except tilings of isosceles triangles with vertex angle greater than or equal to $\frac{\pi}{3}$, has a periodic orbit with period 10.

Finally, we investigate the trihexagonal tiling, which has very complex behavior. We first prove several results about local behavior of trajectories in this tiling (Lemmas 4.2, 4.3, 4.4 and 4.5). Then we use the local results to prove the existence of several periodic trajectories in the tiling (Examples 4.6, 4.9 and 4.13), and then to find infinite families of related drift-periodic trajectories (Propositions 4.7 and 4.10). We show that the limiting member of one such family is dense in the regions it visits:

Corollary 4.11: For the n^{th} family member, the trajectory's intersections with a selected edge are a distance $\frac{1}{2n-1}$ apart, so the limiting trajectory is dense in that edge, and thus is dense in the neighboring tiles.

1.6 Acknowledgements

This research was conducted during the Summer@ICERM program in 2013, where the first author was a teaching assistant and the second, third and fourth authors were undergraduate researchers. We are grateful to ICERM for excellent working condition and the inspiring atmosphere. We thank faculty advisors Sergei Tabachnikov and Chaim Goodman-Strauss for their guidance. We also thank Pat Hooper for sharing his Java code, which we used to model this system.

The two reviewers made suggestions that substantially improved this paper. We especially thank one of them for suggesting the elegant method of proof in Section 2, which replaced our previous methods that used trigonometry and arithmetic.

2 A division of the plane by finitely many lines

In this paper, we consider the case of tiling billiards where the tiling is created by dividing up the plane by lines. The simplest special case is that of finitely many lines. Throughout this section, we assume that there are n lines, and none of the lines are parallel.

Definition 2.1. Identify one of the lines, and name it l_0. For each of the remaining lines, we measure the counter-clockwise angle of intersection with l_0, from the positive horizontal direction. We name them $l_1, \dots l_n$ in order of increasing angle. Define the angle α_i to be the counter-clockwise angle between lines l_i and l_{i+1}, considering the indices modulo n.

Lemma 2.2. $\alpha_0 + \alpha_1 + \cdots + \alpha_{n-1} = \pi$.

Proof. Parallel-translate each of the lines so that they all coincide at a single point. Then the result is clear. □

Definition 2.3. The convex hull of the intersection points of the lines is called the *central zone*. Because we are considering a finite number of non-parallel lines, the number of intersection points is also finite, so the central zone is bounded (Figure 5).

Let θ_i be the angle at the trajectory's i^{th} intersection with a line, measured on the side of the central zone. (This line is l_k, where $k \equiv i \pmod n$.) For convenience, we define the functions $\theta_i(\tau)$, which return this angle for a given trajectory τ.

In any division of the plane containing regions of infinite size, we say that a trajectory *escapes* if it eventually stops refracting across lines and remains in a single region.

If a trajectory neither enters the central zone, nor escapes, for at least $2n$ iterations (refractions), we call the trajectory *good*.

We restrict our analysis in this section to good trajectories. This is a reasonable choice because the requirement to stay outside the central zone isn't taxing: one can "zoom out" until the central zone is of arbitrarily small size. We choose to avoid the central zone because inside the central zone, we cannot guarantee that the trajectory crosses the lines in order, but outside, we can:

Lemma 2.4. *A good trajectory crosses the lines in numerical order: $l_0, l_1, \ldots, l_{n-1}, l_0, l_1$, etc.*

Note that a clockwise trajectory would cross the lines in reverse numerical order; without loss of generality, we may assume that the trajectory travels counter-clockwise.

Proof. Assume the trajectory has just crossed l_i from the side of l_{i-1}. There are four options (see Figure 5): to enter the central zone, to escape, to re-cross l_i, or to cross l_{i+1}. The first two options are impossible by assumption, and the third option is impossible because two lines can only intersect once in the plane. Thus, the trajectory must cross l_{i+1}. □

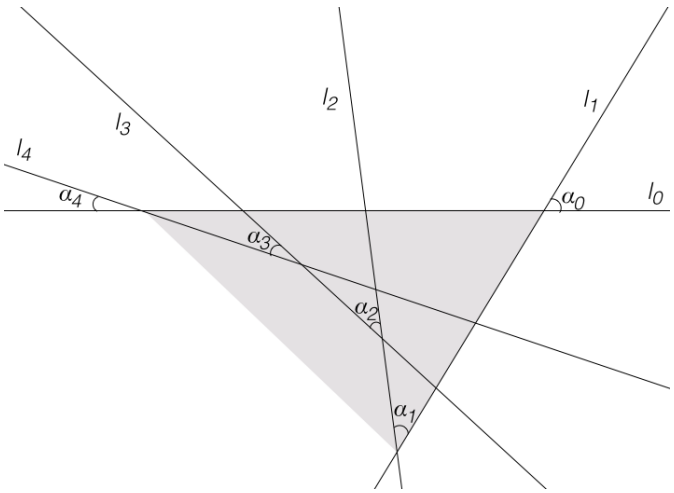

Figure 5: A division of the plane by 5 lines. The central zone is the shaded region.

Lemma 2.5. *The following classical results on planar geometry hold true.*

1. *A composition of reflections across an odd number of lines is a reflection or glide-reflection.*
2. *A translation has a 1-parameter family of parallel fixed lines.*
3. *If the counter-clockwise angle between intersecting lines ℓ_i and ℓ_{i+1} is α_i for $i = 0, 2, \ldots, n-2$, then the composition of reflection through $\ell_0, \ell_1, \ldots, \ell n - 1$ is a counter-clockwise rotation with angle $2(\alpha_0 + \alpha_2 + \ldots + \alpha_{n-2})$.*

Proof. 1. Every planar isometry is either (0) the identity, (1) a reflection in some line, (2) a rotation about a point or a parallel translation by some vector, or (3) a glide-reflection. The parenthetical number indicates the minimum number of reflections across lines necessary to produce the associated isometry.

Reflection across an odd number of lines is orientation-reversing, and thus produces either (1) a reflection or (3) a glide-reflection. Reflection across an even number of lines is orientation-preserving, and thus produces either (0) the identity or (2) a rotation or a translation.

2. In a translation, all of the lines parallel to the translation vector are preserved.

3. If the angle between intersecting lines ℓ_1 and ℓ_2 is α, then the composition of a reflection through ℓ_1 and then ℓ_2 is a rotation of 2α through their intersection point ([1], Chapter III, Theorem 1.12). Furthermore, using pairwise adjustment of reflections, we can reduce a reflection across 4 lines to a reflection across 2 lines: If the angle between intersecting lines ℓ_1 and ℓ_2 is α, and the angle between intersecting lines ℓ_3 and ℓ_4 is β, then the composition of reflections through ℓ_1, ℓ_2, ℓ_3 and ℓ_4 in that order is a rotation of angle $2(\alpha + \beta)$ through some point ([1], Chapter III, Theorem 4.1). By repeatedly reducing reflections through 4 lines to reflections through 2 lines and applying this result, we obtain the desired statement.

□

Theorem 2.6. *For $n \geq 3$ odd, there is always a trajectory of period $2n$. A periodic direction is given by the initial angle (measured between the trajectory and l_0, on the same side as the intersection of l_0 and l_1)*

$$\theta = \alpha_1 + \alpha_3 + \ldots + \alpha_{n-2}. \tag{1}$$

Proof. Let T be the composition of reflections in $l_0, \ldots, l_{n-1}$. Any good trajectory will circle the central zone before it gets back to l_0, reflecting across the n lines in order twice, so we consider the transformation T^2. Since n is odd, by Lemma 2.5 part 1 T is either a reflection or a glide-reflection, so T^2 is either the identity or a translation, respectively. If T^2 is the identity, then there is a two-parameter family of periodic trajectories. If T^2 is a translation, by Lemma 2.5 part 2 there is a 1-parameter family of parallel fixed lines. Choose any such line that does not intersect the central zone; this provides a periodic trajectory. Such a trajectory circles the central zone once, refracting across each line twice, so it has period $2n$.

A calculation in arithmetic shows that, for the value of θ in (1), the trajectory returns to the same starting angle, and a Law of Sines argument shows that the distance is preserved, so the trajectory is periodic. Thus, this angle describes a periodic direction. We omit the calculation. □

Corollary 2.7. *Let $n \geq 3$ be odd. If all of the angles are equal, i.e. $a_i = \pi/n$ for all n, then the angle condition (1) reduces to $\theta_0 = \frac{n-1}{2n}\pi$, which gives a periodic direction.*

Corollary 2.7 applies in the case that the lines are the extensions of the edges of a regular polygon, or any equiangular polygon.

Proposition 2.8. *Let $n \geq 2$ be even, let T be the composition of reflections through $l_0, \ldots, l_{n-1}$, and consider the following angle condition:*

$$0 = \alpha_0 - \alpha_1 + \alpha_2 - \alpha_3 + \cdots + \alpha_{n-4} - \alpha_{n-3} + \alpha_{n-2} - \alpha_{n-1}. \tag{2}$$

T is a rotation by π and T^2 is the identity if and only if (2) is satisfied.

Proof. By Lemma 2.2, the sum of all the α_i is π, so an equivalent statement to (2) is

$$\alpha_0 + \alpha_2 + \ldots + \alpha_{n-2} = \alpha_1 + \alpha_3 + \ldots + \alpha_{n-1} = \pi/2.$$

By Lemma 2.5 part 3, a composition of reflections through $l_0, l_1, \ldots, l_{n-1}$ is a rotation by angle $\alpha_0 + \alpha_2 + \ldots + \alpha_{n-2}$, so T is a rotation by angle $2(\pi/2) = \pi$ if and only if (2) is satisfied. Any good trajectory will circle the central zone before it gets back to l_0, reflecting across the n lines in order twice, so we consider the transformation T^2, which is a rotation of angle 2π (the identity) if and only if (2) is satisfied. □

Corollary 2.9. *If $\theta_n(\tau) = \theta_0(\tau)$, then $\theta_{i+n}(\tau) = \theta_i$ for all $i \geq 0$.*
If $\theta_n(\tau) = \theta_0(\tau)$, then τ is periodic.

Theorem 2.10. *If (2) is satisfied, then every good trajectory is periodic. If (2) is not satisfied, then no good trajectory is periodic.*

Proof. If (2) is satisfied, then by Proposition 2.8, T^2 is the identity, so it has a two-parameter family of fixed lines; as in Theorem 2.6, this yields a periodic trajectory of period $2n$.

If (2) is not satisfied, then by Lemma 2.8, T is a nontrivial rotation, so T^2 is also a rotation. A nontrivial rotation has no fixed lines, so no direction is preserved, and no trajectory is periodic. □

We also consider the special case where all of the lines coincide, so the central zone is just the point of coincidence.

Corollary 2.11. *Divide the plane by $n \geq 2$ lines coinciding at a point p, and consider a trajectory τ with initial angle θ.*

1. *If n is odd and (1) is satisfied, then τ is periodic.*
2. *If n is even and (2) is satisfied, then every non-escaping trajectory is periodic; if (2) is not satisfied, then every trajectory escapes.*

These follow directly from Theorem 2.6 and Theorem 2.10.

The above results show when periodic trajectories exist, and how to construct them. Now we will show that when a trajectory is not periodic, it can spiral.

Definition 2.12. A periodic trajectory is *stable* if, when the initial angle is changed by some arbitrarily small angle, the the trajectory hits the same series of edges and the returns to its starting angle and location.

Proposition 2.13. *Consider a good trajectory τ and suppose that $\theta_0(\tau) = \theta_n(\tau)$. The trajectory is periodic. If n is even, the trajectory is stable. If n is odd, the trajectory is not stable; the perturbed trajectory spirals.*

Proof. Since $\theta_n = \theta_0$, the trajectory is periodic by Corollary 2.9, so it suffices to examine the stability.

Let τ' be the trajectory that starts in the same place as τ, and has initial angle $\theta_0(\tau') = \theta_0(\tau) + \epsilon$, where ϵ is small enough (positive or negative) so that τ' is still a good trajectory.

Then we have

$$\begin{aligned}
\theta_0(\tau') &= \theta_0(\tau) + \epsilon \\
\theta_1(\tau') &= \theta_1(\tau) - \epsilon \\
&\vdots \\
\theta_i(\tau') &= \theta_i(\tau) + (-1)^i\epsilon.
\end{aligned}$$

If n is even, then $\theta_n(\tau') = \theta_n(\tau) + \epsilon = \theta_0(\tau')$. Since the perturbation τ' of τ hits the same series of edges and returns to its starting angle and location, τ is stable.

If n is odd, then $\theta_n(\tau') = \theta_n(\tau) - \epsilon = \theta_0(\tau') - 2\epsilon$. By Corollary 2.9, we still have $\theta_{2n} = \theta_0$, so τ' spirals. □

3 Triangle Tilings

In this section, we investigate tiling billiards where the plane is cut up by infinitely many lines that divide the plane in a very regular way, into congruent triangles. The behavior of the system in some cases is predictable and elegant, perhaps because of the substantial symmetry.

Definition 3.1. A *triangle tiling* is a covering of the Euclidean plane with non-overlapping congruent copies of the *tiling triangle* so that the tiling is a grid of parallelograms with parallel diagonals.

The valence of every vertex of a triangle tiling is 6. Note that the $30°$-$60°$-$90°$ triangle tiling in Figure 2 is *not* a triangle tiling by our definition. Since every vertex of a triangle tiling is the intersection of three lines, we have the following result:

Corollary 3.2 (to Corollary 2.11)**.** *Every triangle tiling has a trajectory of period 6 around each vertex.*

Lemma 3.3 (Angle Adding Lemma)**.** *Consider a trajectory that consecutively meets the two legs of the tiling triangle that form angle α. If the angle that the trajectory makes with the first leg, on the side away from α, is θ, then the angle that the trajectory makes with the second leg, on the side away from α, is $\theta + \alpha$.*

Proof. If a trajectory hits the legs of angle α, then it forms a triangle, where one angle is α and another is the initial angle θ of the trajectory. So the exterior angle of the third angle must be $\theta + \alpha$, as shown in Figure 6. □

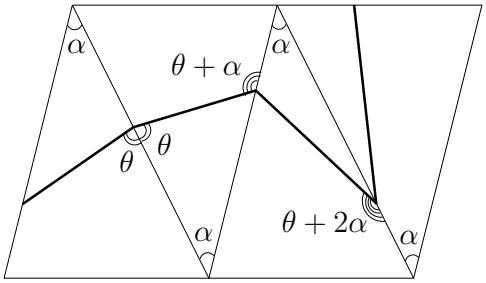

Figure 6: The angle a trajectory makes with a leg of a tiling triangle increases by α on the side of the trajectory away from the angle α.

3.1 Isosceles triangle tilings

Theorem 3.4. *Consider an isosceles triangle tiling, and let the vertex angle be α.*

1. *All trajectories are either periodic or drift-periodic.*
2. *Consider a trajectory making angle $\theta < \alpha$ with one of the congruent legs. Let $n \in \mathbb{N}$ be the unique value such that $\pi - \alpha \leq \theta + n\alpha < \pi$. If n is even, the maximum period of a drift-periodic trajectory is $2n + 4$ and the maximum period of a periodic trajectory is $2n + 2$; if n is odd, the maximum period of a drift-periodic trajectory is $2n + 2$ and the maximum period of a periodic trajectory is $2n + 4$.*

Proof. 1. Call each line containing the bases of the isosceles triangles the *base line*. Note that an isosceles triangle tiling is reflection-symmetric across the base lines, and therefore so are the trajectories. So if a trajectory crosses the same base line in two places, then it must make a loop upon reflection across that line; the trajectory is periodic (Figure 7a). If a trajectory crosses two distinct base lines, then upon reflection across either of these lines, the trajectory will hit yet another base line, in the same place and at the same angle on the side of a triangle corresponding to the previous place the trajectory met a base line (Figure 7b); the trajectory is drift-periodic.

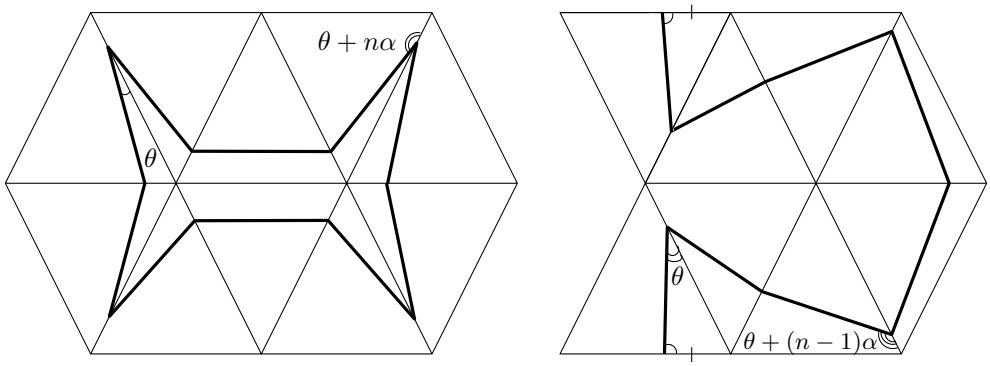

Figure 7: Two trajectories in an isosceles triangle tiling: (a) a periodic trajectory and (b) a drift-periodic trajectory. Note that these trajectories are reflection-symmetric across the base line.

Furthermore, every trajectory falls into one of these two cases because a trajectory cannot travel indefinitely without crossing a base: each time a trajectory goes from leg to leg in the tiling, by the Angle Adding Lemma α is added to the angle the trajectory makes with the next leg. Eventually, this angle is greater than or equal to $\pi - \alpha$ and the trajectory meets a base. So every trajectory is either periodic or drift-periodic.

2. Note that by the Angle-Adding Lemma, θ is the smallest angle that the trajectory makes with the edges. By the definition of n, $\theta + n\alpha$ is the largest angle a trajectory can make with a leg before the trajectory meets a base line. Suppose that a trajectory meets this maximum number of legs n. If n is even, then the trajectory meets another base line after making the angle $\theta + n\alpha$ with a leg and, by the reflection symmetry of the tiling across the base lines, is drift-periodic. By the Angle Adding Lemma and reflection symmetry, a drift-periodic trajectory must have $2n$ points where the trajectory makes the angles $\theta + \alpha, \theta + 2\alpha, \ldots, \theta + n\alpha$. Add to this the 4 points when the trajectory is traveling to and from a base edge, and the maximum period of a drift-periodic trajectory is $2n + 4$. Similarly, the maximum period of a periodic trajectory is $2(n-1) + 4 = 2n + 2$. If n is odd, then the trajectory meets a base line a second time after making the angle $\theta + n\alpha$ with a leg and is periodic; the maximum period of a drift-periodic trajectory is $2(n-1) + 4 = 2n + 2$ and the maximum period of a periodic trajectory is $2n + 4$. □

Theorem 3.4 shows that every trajectory in an isosceles triangle tiling is either periodic or drift-periodic, and we might wonder if all isosceles triangles yield both. No: we know (Corollary 3.2) that every triangle tiling has a periodic trajectory, but Theorem 1.1 shows that the equilateral triangle tiling (a special case of an isosceles triangle) does *not* have a drift-periodic trajectory. We conjecture that this is not the only exception:

Conjecture 3.5. *An isosceles triangle tiling has an escaping trajectory if and only if its vertex angle is* not *of the form* $\pi/(2n+1)$.

3.2 Right triangle tilings

Notation: We assume that a *right triangle tiling* is a covering of the Euclidean plane with non-overlapping congruent right triangles so that the tiling has axis-parallel perpendicular edges and the hypotenuses are the negative diagonals of the rectangles formed by the perpendicular edges. We refer to a tiling triangle that lies below its hypotenuse as a *lower tiling triangle*, and to a tiling triangle that lies above its hypotenuse as an *upper tiling triangle*. In any right triangle tiling, α is the smallest angle in the right triangle, and is opposite the horizontal edge. The length of the hypotenuse of the tiling triangle is 1.

Lemma 3.6. *In a right triangle tiling, if a trajectory never meets two perpendicular edges in a row, then the trajectory is unbounded.*

Proof. Consider a trajectory that never meets two perpendicular edges in a row as it passes through a lower tiling triangle, then meets the hypotenuse (Figure 8 (a)). The trajectory then passes through the upper tiling triangle and crosses either the top or right edge. Either way, it will enter another lower tiling triangle, meet the hypotenuse, then go up or right once again. So the trajectory always travels up and right (or in the symmetric case, down and left) and escapes to infinity. □

Theorem 3.7. *Every right triangle tiling has an escaping trajectory.*

Proof. First, we show that if a trajectory bisects a hypotenuse, then it bisects the hypotenuse of every tiling triangle it enters. Then, we show that if a trajectory bisects a hypotenuse, then the trajectory iescapes.

Let p be the midpoint of a hypotenuse, p' be the reflection of p across the horizontal edge above p, and p'' be the reflection of p' across the vertical edge to the right of p' (see Figure 8 (b)). By symmetry, p' is the midpoint of the hypotenuse, and also by symmetry, a trajectory through p that crosses the horizontal edge must pass through p'. By a similar argument, p'' is the midpoint of the hypotenuse and a trajectory through p' that crosses the vertical edge must pass through p''.

Hence the trajectory cannot meet two perpendicular edges in a row; by Lemma 3.6, the trajectory escapes. □

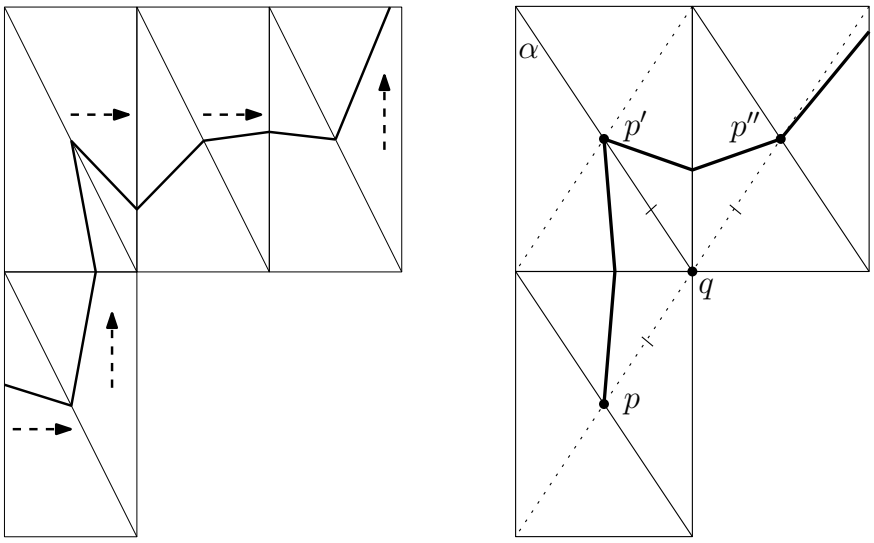

Figure 8: (a) A trajectory that never meets two perpendicular edges in a row only travels up and to the right. (b) If a trajectory bisects a hypotenuse, it will bisect every hypotenuse.

Lemma 3.8. *If a trajectory meets a hypotenuse below (above) its midpoint, the trajectory will continue to meet each hypotenuse below (above) its midpoint until it meets two perpendicular edges in a row, at which point the trajectory will begin to meet hypotenuses above (below) their midpoints.*

Proof. Let the trajectory meet a hypotenuse below the midpoint in such a way that it next meets a vertical leg, whose lower endpoint is P and upper endpoint is Q, then meets another hypotenuse, whose midpoint we name R (Figure 9). Consider $\triangle PQR$. To meet the hypotenuse above the midpoint, the trajectory would have to meet QR. However, this is impossible because, by reflection, the trajectory meets PR.

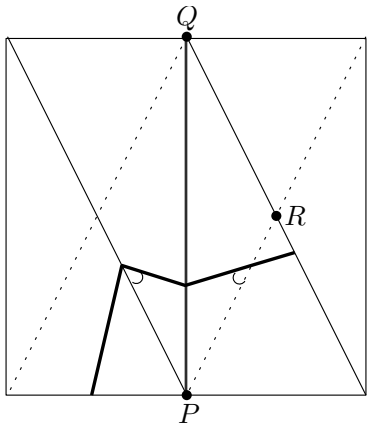

Figure 9: A trajectory that meets a hypotenuse below its midpoint will continue to meet hypotenuses below their midpoints.

Suppose a trajectory meets hypotenuses below the midpoint as described above, but then meets both legs of a tiling triangle before meeting another hypotenuse (Figure 10). Construct the positive diagonals of the tiling. Let p, p', and p'' be the points where the trajectory meets the first, second, and third diagonals, respectively, and let q be the shared endpoint of the first and third hypotenuses. (Recall that we assume the hypotenuse has length 1.) By symmetry, $|pq| = |qp''|$. So if $|pq| < \frac{1}{2}$, then $|qp''| < \frac{1}{2}$, so the trajectory meets the third hypotenuse above the midpoint.

The same argument with the direction of the trajectory reversed applies to trajectories meeting the hypotenuse above the midpoint. □

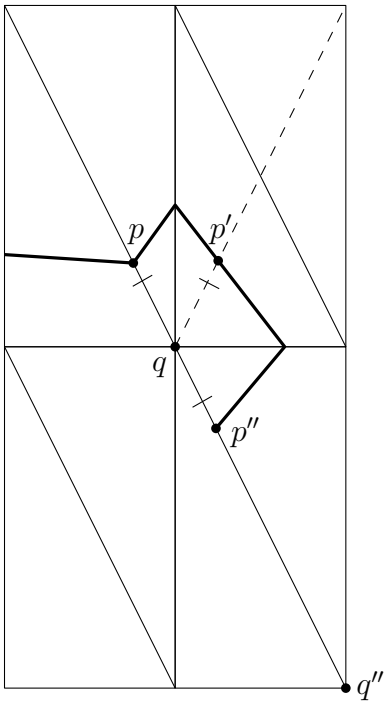

Figure 10: When a trajectory meets two perpendicular edges in a row, it switches from meeting hypotenuses below their midpoints (p) to meeting them above their midpoints (p'').

In Theorem 3.4, we showed that in an isosceles triangle tiling, *every* trajectory is periodic or drift-periodic. We now show (Theorem 3.9) that some rational right triangle tilings always have *at least one* drift-periodic trajectory, and we conjecture that this is true for all rational right triangle tilings.

Theorem 3.9. *If $\alpha = \frac{\pi}{2n}$ for some $n \in \mathbb{N}$, then a drift-periodic trajectory exists.*

Proof. Construct a trajectory that perpendicularly bisects the short leg of a right tiling triangle (Figure 11). The trajectory bisects the hypotenuse of the triangle, meeting it at angle α. By the Angle Adding Lemma, there exists a hypotenuse where the trajectory meets at angle $(2n-1)\alpha = \pi - \alpha$. Since the trajectory bisects a hypotenuse, by Proposition 3.7, the trajectory bisects every hypotenuse it meets, so the trajectory perpendicularly bisects the short leg of the upper triangle whose hypotenuse the trajectory meets at angle $(2n-1)\alpha$. Since the trajectory meets an edge at a corresponding point and at the same angle as where it started, the trajectory is drift-periodic. □

Note that the trajectory will also bisect the long leg of a right tiling triangle so we could also begin our construction there, replacing α with $\frac{\pi}{2} - \alpha$ and following the same argument.

In fact, our experiments suggest that Theorem 3.9 holds for all rational right triangles:

Conjecture 3.10. *Every right triangle tiling has a drift-periodic trajectory.*

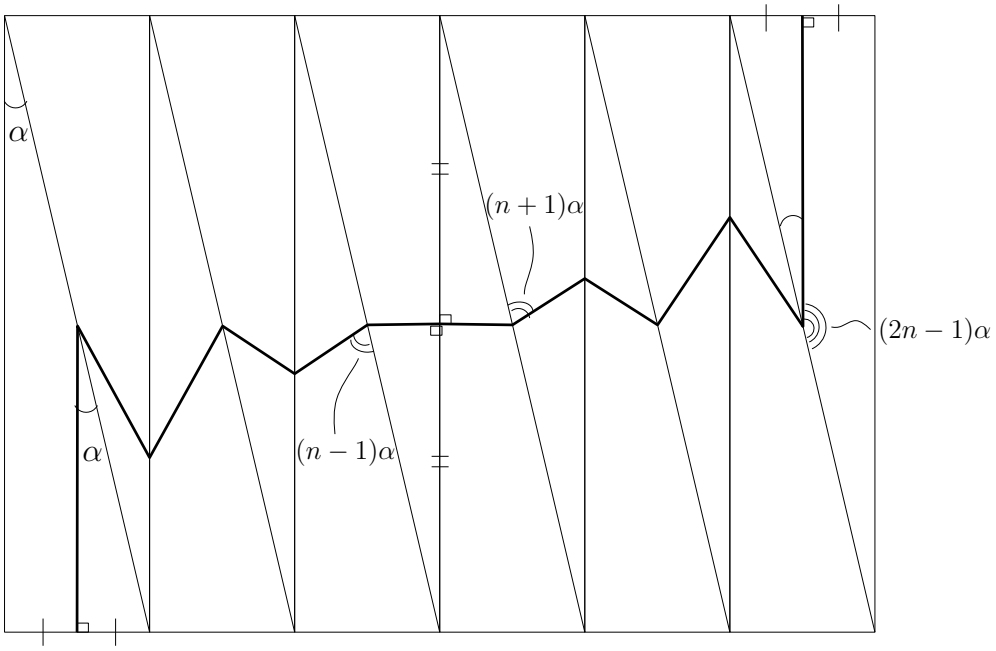

Figure 11: A trajectory that perpendicularly bisects the legs of a right tiling triangle must be drift-periodic if $\alpha = \frac{\pi}{2n}$, $n \in \mathbb{N}$.

Many questions remain open regarding periodic orbits of right triangle tilings. During computer experimentation, we noticed that there appears to be a bound on the period of an orbit contained in a single row of the tiling (Figure 12). All periodic orbits observed with larger periods crossed more than one row and remained in each row for the same number of refractions (± 2) as occur in the maximum one-row periodic orbit. However, not every possible number of rows was crossed in a periodic orbit. We would like to find a rule for how many rows will be crossed in a periodic orbit, and determine if there is a bound on the periods in a right triangle tiling.

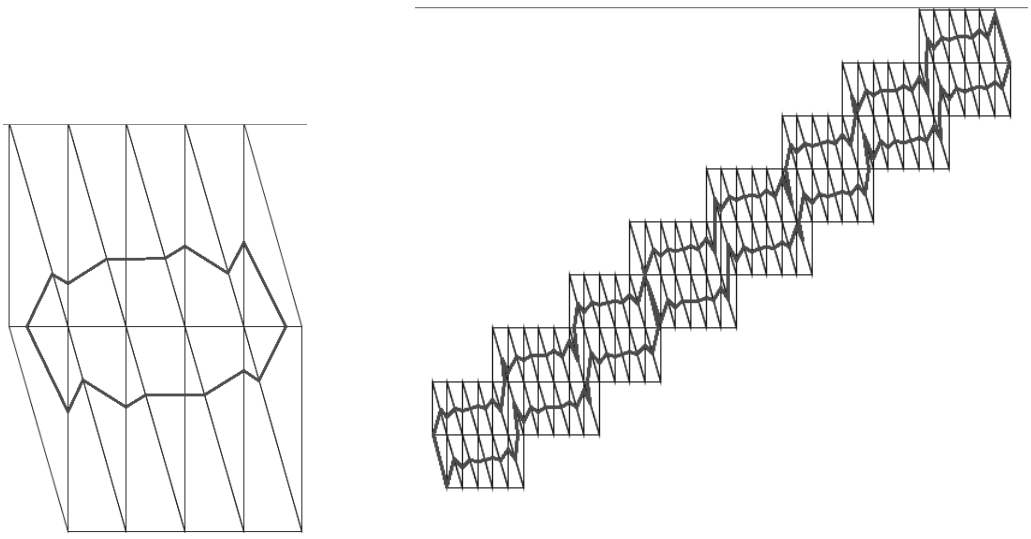

Figure 12: (a) The largest periodic orbit contained in a single row. (b) A longer periodic orbit. Note that each row resembles the one-row periodic orbit.

3.3 Periodic trajectories on general triangle tilings

Theorem 3.11. *Every triangle tiling, except tilings of isosceles triangles with vertex angle greater than or equal to $\frac{\pi}{3}$, has a periodic trajectory with period 10.*

Proof. Let α, β be two angles of the tiling triangle and θ be the initial angle the trajectory makes with the side of the tiling triangle between α and β, on the α side of the trajectory. In Figure 13, we see a ten-periodic trajectory for a generic triangle tiling. If each of the labeled angles is between 0 and π, then there exists a trajectory around two groups of intersecting lines making the angles α, β, and $\pi - \alpha - \beta$. When we add edges so that these intersecting lines become a tiling of triangles with angles α, β, and $\pi - \alpha - \beta$, we can shrink the periodic trajectory with period 10 so that it fits within the bounds of the triangles.

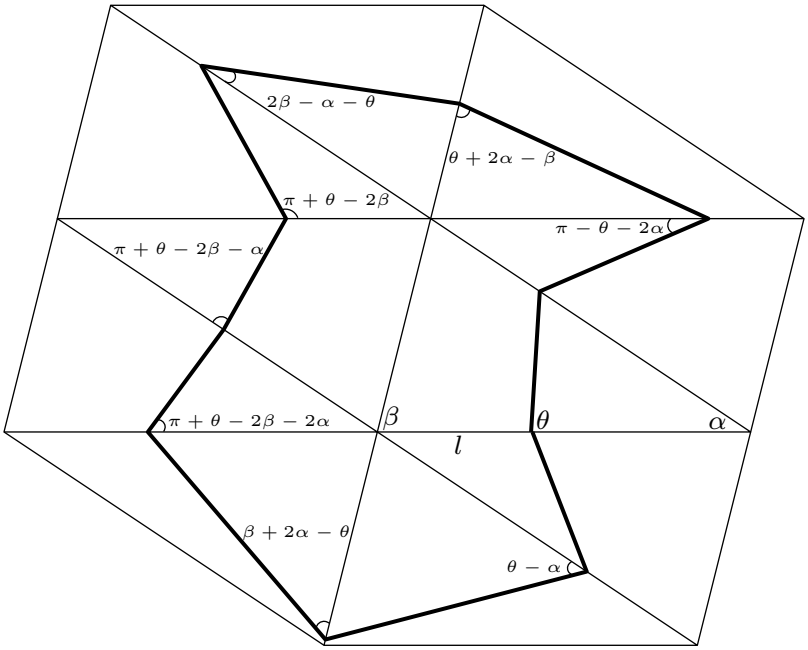

Figure 13: If each of the labeled angles is positive, then this ten-periodic trajectory exists.

If we start with a system of inequalities based on every angle in the trajectory being positive, we can reduce it to the following system, which implies that a ten-periodic trajectory exists:

$$\begin{cases} 0 & < \theta \\ \beta - 2\alpha & < \theta \\ 2\beta + 2\alpha - \pi & < \theta \\ \alpha & < \theta \end{cases} \qquad \begin{cases} \theta < \pi \\ \theta < \pi - 2\alpha \\ \theta < 2\beta - \alpha \\ \theta < \beta + 2\alpha. \end{cases}$$

By combining each inequality on the left with each inequality on the right, we can reduce the system to the following three inequalities that depend only on α and β, and not on θ:

$$\begin{cases} \pi & > \beta + 2\alpha \\ \frac{\pi}{3} & > \alpha \\ \beta & > \alpha. \end{cases}$$

We graph these in Figure 14. The region of values of α and β where there exists a periodic trajectory of period 10 is shaded dark gray, and does not contain its boundaries. Since this region contains all β between 0 and π, every scalene triangle tiling has a periodic trajectory of period 10. However, this is not so for every isosceles triangle tiling. Isosceles triangles lie on the lines $\alpha = \beta$, $\pi = 2\alpha + \beta$ (both dashed), and $\pi = 2\beta + \alpha$ (dotted). The two dashed lines coincide with the boundaries of the region where there exists a periodic trajectory of period 10. The third and dotted

line is contained in the region of acceptable values when $\pi/3 < \beta < \pi/2$ and $\alpha < \pi/3$. In other words, an isosceles triangle only has a ten-periodic trajectory if its vertex angle is less than $\frac{\pi}{3}$, and a base line of the tiling must cross the interior of the periodic trajectory of period 10.

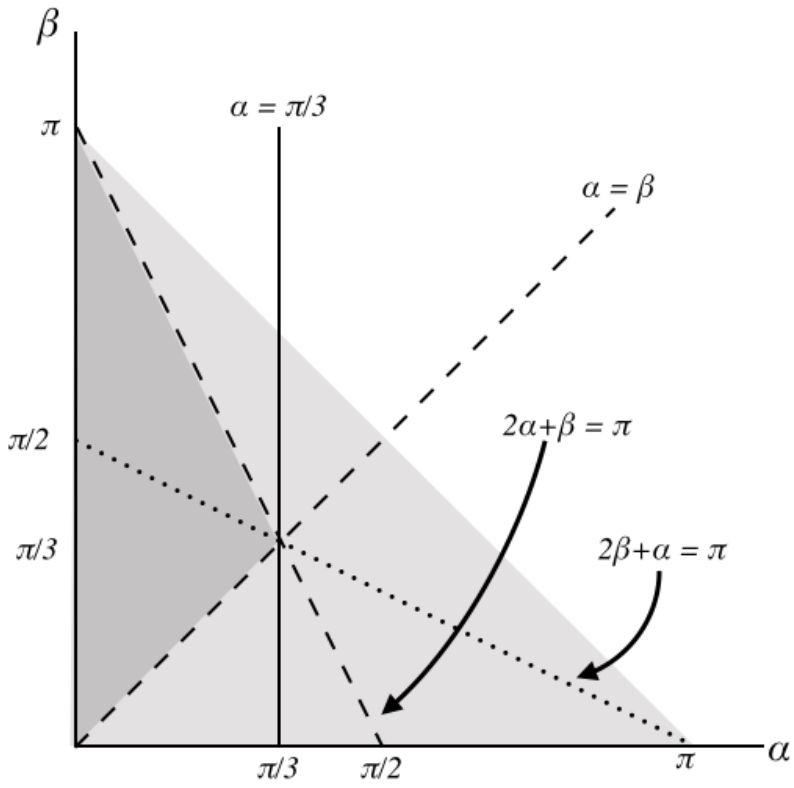

Figure 14: The system of inequalities $\pi > \beta + 2\alpha, \pi > 2\beta + \alpha$, and $\beta > \alpha$. The (open) light gray region represents all possible triangles. The (open) dark gray region represents all triangles with a period-10 trajectory. The dashed and dotted lines represent isosceles triangles. The portion of the dotted line $\pi = 2\beta + \alpha$ in the dark gray region represents the set of α, β where an isosceles triangle has a ten-periodic trajectory.

The above shows that the trajectory returns to the same angle. We can show that the location (distance along the edge) is also the same via repeated application of the Law of Sines.

We can construct a ten-periodic trajectory by choosing a value for l, the distance of the trajectory from the vertex of angle β along the side between α and β where the trajectory makes the angle θ (Figure 13), such that our system of inequalities holds.

For example, if $\alpha = \frac{\pi}{5}$ and $\beta = \frac{3\pi}{10}$, then θ must be between $\frac{\pi}{5}$ and $\frac{2\pi}{5}$. Let $\theta = \frac{3\pi}{10}$. Then $0 < l < \frac{2}{3+\sqrt{5}}$, when the edge of the tiling triangle between angles α and β has length 1.

□

Conjecture 3.12. *There exist triangle tilings with periodic trajectories of arbitrary length.*

For example, the scalene triangle tiling in Figure 15 has a periodic trajectory of period 34.

Conjecture 3.13. *In a triangle tiling, every periodic trajectory has a period of the form $4n + 2$.*

In Corollary 2.13, we showed that for a division of the plane by an odd number of lines, a trajectory can spiral. We do not observe this behavior on triangle tilings:

Conjecture 3.14. *Trajectories on triangle tilings never spiral.*

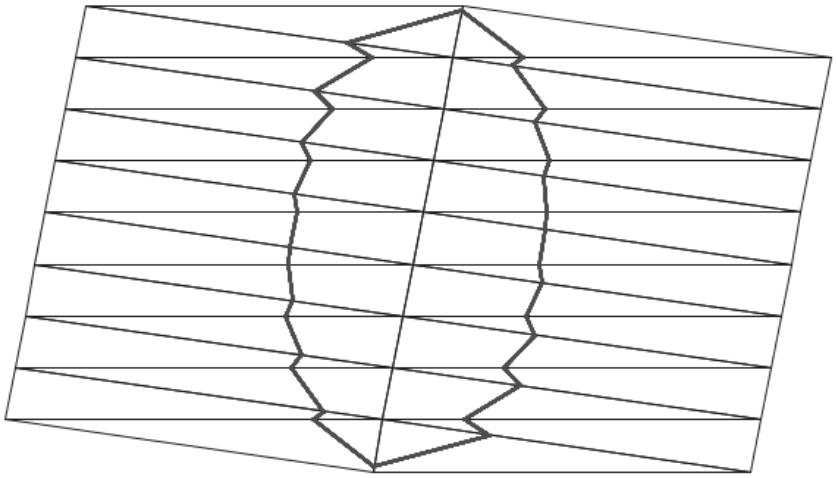

Figure 15: The triangle tiling with angles $8°, 79°$, and $93°$ and a trajectory of period 34.

4 The Trihexagonal Tiling

The equilateral triangle tiling and the regular hexagon tiling have very simple dynamics (Theorem 1.1), but the composition of these two tilings into the trihexagonal tiling offers a myriad of interesting dynamics, which we explore in this section. As mentioned in the Introduction, trajectories in the trihexagonal tiling are very unstable; a tiny change in the direction can transform a periodic trajectory into a trajectory that escapes. In this sense, the trihexagonal tiling has similar behavior to inner billiards, where a tiny change in the direction of a trajectory on the square table, from a rational to an irrational slope, will transform a periodic trajectory into a dense trajectory.

Our goal was to find the periodic trajectories and drift-periodic trajectories of the trihexagonal tiling and analyze their stability. The dynamics of this tiling turn out to be complicated and interesting, so we analyze the local behavior of trajectories around single vertices or tiles (Lemmas 4.2-4.5), and then give explicit examples of periodic trajectories on this tiling (Examples 4.6, 4.9, and 4.13). We also construct two families of drift-periodic trajectories (Propositions 4.7 and 4.10), and for one of these families, we show that the limiting trajectory is dense in some edges of the tiling (Corollary 4.11).

Definition 4.1. The *trihexagonal tiling* is the edge-to-edge tiling where an equilateral triangle and a regular hexagon meet at each edge. Examples showing large areas of this tiling are in Figures 22-24. We assume that each of the edges in the tiling has unit length.

We assume that a trajectory τ starts on an edge of the tiling, at a point p_1, and its subsequent intersections with edges are p_2, p_3, etc. The distance x_i from p_i to a vertex is not clearly defined; it could be x_i or $1 - x_i$. It is most convenient for us to use triangles, so we choose to define x_i as follows: Every edge of the trihexagonal tiling is between an equilateral triangle and a hexagon. In the equilateral triangle, τ goes from p_i on edge e_i to p_{i+1} on an adjacent edge e_{i+1}, thus creating a triangle whose edges are formed by e_i, e_{i+1} and τ. Let x_i be the length of the triangle's edge along e_i and let x_{i+1} be the length of the triangle's edge along e_{i+1}.

Define the angle α_i to be the angle between τ and an edge of the tiling at p_i, where α_i is between the trajectory and the edge with length x_i as defined above. The *initial angle* of a trajectory is the angle α_1; since we frequently use this angle, we denote it by α.

4.1 Local geometric behavior in the trihexagonal tiling

First, we state four lemmas in elementary geometry about local trajectory behavior in the tiling. In the next section, we use these lemmas to prove periodicity of several periodic and drift-periodic trajectories in the tiling.

Lemma 4.2 (The Trajectory Turner)**.** *Consider a trajectory crossing the edges of the tiling at p_1, p_2, p_3, p_4 where segments $\overline{p_1p_2}$ and $\overline{p_3p_4}$ lie in distinct triangles, and segment $\overline{p_2p_3}$ lies in the hexagon adjacent to both triangles. Then $x_1 = x_4$. Also, $\alpha_4 = \pi - \alpha$.*

Proof. We include a proof of this elementary result because we can use a folding argument (see Theorem 1.1 in the Introduction) even though the tiling is *not* reflection-symmetric across the edges of the tiling.

In Figure 16, we fold the triangles onto the hexagon, and find that lengths x_1 and x_4 measure distances that fold up to the same segment, so they are equal. The angles at p_1 and p_2 fold up to make a straight line, so $\alpha_4 = \pi - \alpha_1$. □

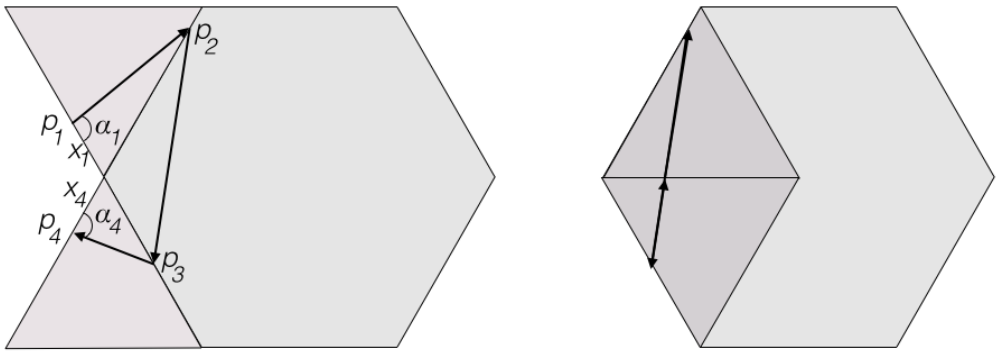

Figure 16: The Trajectory Turner, proven via a folding argument

Lemma 4.3 (The Quadrilateral)**.** *In a regular hexagon $ABCDEF$, suppose a trajectory passes from side AB to side CD, crossing AB at p_1 and CD at p_2. If the angle at p_1, measured on the same side of the trajectory as B, is $\pi - \alpha$, then $x_2 = \frac{\sin(\alpha)(2x_1+1)+\sqrt{3}\cos(\alpha)}{2\sin(\alpha-\frac{\pi}{3})}$. Also, $\alpha_2 = \alpha - \pi/3$.*

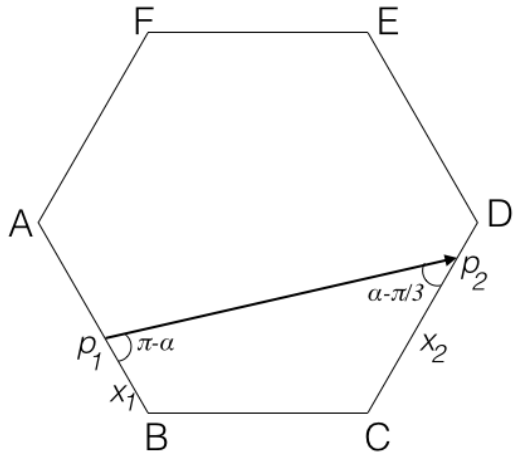

Figure 17: The Quadrilateral

Lemma 4.4. The Quadrilateral-Triangle *Let ABCDEF, p_1, p_2 and x_1 be as in The Quadrilateral. Consider equilateral triangle CDT, and let p_3 be the point where the trajectory meets CT (Figure 18 (a)).*

Then $x_3 = \frac{1}{2} + x_1 + \frac{\sqrt{3}}{2}\cot\alpha$. Also, $\alpha_3 = \pi - \alpha$.

Lemma 4.5. The Pentagon *In a regular hexagon $ABCDEF$, suppose a trajectory passes from side AB to side DE , crossing AB at p_1 and DE at p_2 (Figure 18 (b)). If the angle at p_1, measured on the same side of the trajectory as B, is $\pi - \alpha$, then $x_2 = x_1 + \sqrt{3}\cot\alpha$. Also, $\alpha_2 = \alpha$.*

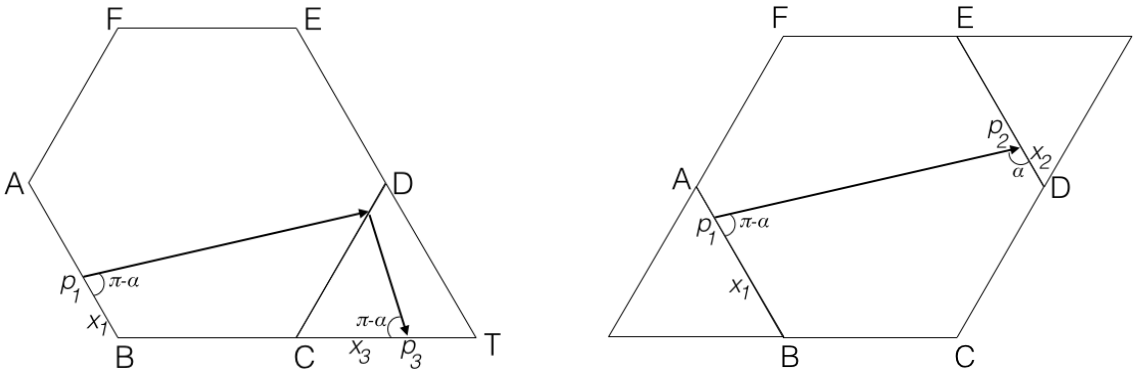

Figure 18: (a) The Quadrilateral-Triangle (b) The Pentagon

4.2 Periodic and drift-periodic trajectories in the trihexagonal tiling

Using our results about local behavior in the trihexagonal tiling, we will now prove the existence of certain periodic and drift-periodic trajectories. In each case, we first give a simple periodic trajectory (Examples 4.6 and 4.9), and then show how a perturbation of the simple trajectory yields a family of drift-periodic trajectories with arbitrarily large period (Propositions 4.7 and 4.10).

Example 4.6. There is a 6-periodic trajectory intersecting all edges of the tiling at angle $\frac{\pi}{3}$ (Figure 19). This trajectory circles three lines forming a regular triangle, so by Corollary 2.7, an initial angle of $\frac{3-1}{2\cdot 3}\pi = \frac{\pi}{3}$ makes the trajectory periodic.

This trajectory is stable under parallel translations for any $0 < x_1 < 1$; see the dashed trajectory in Figure 19.

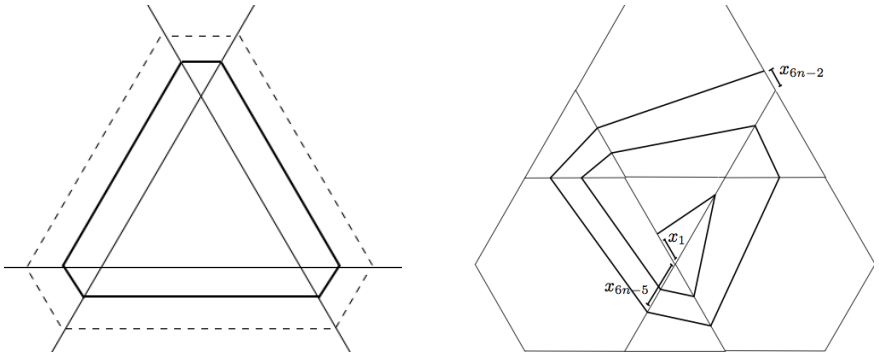

Figure 19: (a) The period-6 trajectory of Example 4.6, (b) One period of the drift-periodic trajectory in Proposition 4.7 where $n = 2$

If we perturb the periodic trajectory in Figure 19 (a), we obtain a family of drift-periodic trajectories. One period of such a trajectory is in Figure 19 (b). We describe this family in Proposition 4.7.

Proposition 4.7. *For any $n \in N$, there is a drift-periodic trajectory of period $6n$ that intersects each edge of the tiling a maximum of n times.*

Proof. Let $\alpha = \pi - \tan^{-1}\left(\frac{3n\sqrt{3}}{3n-2}\right)$. (This angle is less than, and approaches, $2\pi/3$.) Then

$$\cot\alpha = \frac{-(3n-2)}{3n\sqrt{3}} = \frac{-\frac{1}{2}(3n-2)}{(3n-2)\frac{\sqrt{3}}{2}+\sqrt{3}}.$$

We wish to show that $x_{6n+1} = x_1$ and $\alpha_{6n+1} = \alpha$.

By the Pentagon Lemma, $x_{6n+1} = x_{6n} + \sqrt{3}\cot(\pi - \alpha_{6n})$ and $\alpha_{6n+1} = \pi - \alpha_{6n}$.

By the Quadrilateral Triangle Lemma, $x_{2k+2} = x_{2k} + \frac{1}{2} + \frac{\sqrt{3}}{2}\cot(\pi - \alpha_{2k})$ and $\alpha_{2k+2} = \alpha_{2k}$ for $k \geq 3$. We apply this result $3n-2$ times to x_{6n} and α_{6n} to yield $\alpha_{6n+1} = \pi - \alpha_4$ and

$$\begin{aligned} x_{6n+1} &= x_{6n} + \sqrt{3}\cot(\pi - \alpha_{6n}) \\ &= x_4 + (3n-2)\left(\frac{1}{2} + \frac{\sqrt{3}}{2}\cot(\pi - \alpha_4)\right) + \sqrt{3}\cot(\pi - \alpha_4). \end{aligned}$$

By the Trajectory Turner Lemma, $x_4 = x_1$ and $\alpha_4 = \pi - \alpha_1 = \pi - \alpha$, so $\alpha_{6n+1} = \alpha$ and

$$\begin{aligned} x_{6n+1} &= x_1 + (3n-2)\left(\frac{1}{2} + \frac{\sqrt{3}}{2}\cot\alpha\right) + \sqrt{3}\cot\alpha \\ &= x_1 + \frac{1}{2}(3n-2) + \cot\alpha\left((3n-2)\frac{\sqrt{3}}{2} + \sqrt{3}\right) = x_1, \end{aligned}$$

by substituting the expression for $\cot\alpha$.

□

Remark 4.8. We can take the limit of the initial angle α as $n \to \infty$:

$$\lim_{n\to+\infty}\alpha = \lim_{n\to+\infty}\pi - \tan^{-1}\left(\frac{3n\sqrt{3}}{3n-2}\right) = \frac{2\pi}{3}.$$

This implies that our drift-periodic trajectory is converging to the periodic trajectory in Example 4.6. Our angle α is bounded below by $\alpha = \pi - \tan^{-1}(3\sqrt{3}) \approx 0.56\pi$ and above by $\alpha = \frac{2}{3}\pi$.

Example 4.9. There is a 12-periodic trajectory that intersects the edges of the tiling at angles $\frac{\pi}{2}$ and $\frac{\pi}{6}$ (Figure 20 (a)).

This trajectory is stable under parallel translations: As long as the trajectory intersects the edge of the central hexagon perpendicularly, any value of x_1, with $0 < x_1 < \frac{1}{2}$, produces a parallel periodic trajectory. An example is shown as a dashed trajectory in Figure 20 (a).

Proposition 4.10. *For any $n \geq 2$, there is a drift-periodic trajectory with period $12n-6$ that intersects each edge of a tiling a maximum of n times (Figure 21).*

Proof. Given n, choose $\alpha = \tan^{-1}((6n-3)\sqrt{3})$ as the initial angle of the trajectory. (This angle is less than, and approaches, $\pi/2$.) In order to avoid hitting a vertex, we need to carefully choose p_1. The following calculations show that given any n, there is an $x_1 > 0$ so that p_1 can be placed a distance x_1 from the midpoint and create the drift-periodic trajectory.

By the Pentagon Lemma, we calculate $x_{13} = x_1 + 3\sqrt{3}\cot\alpha$. This gives $|p_1p_{13}| = 3\sqrt{3}\cot\alpha$, and in general, since $\alpha = \tan^{-1}((6n-3)\sqrt{3})$, we have

$$|p_{12k+i}p_{12(k+1)+i}| = 3\sqrt{3}\cot\alpha = \frac{3\sqrt{3}}{(6n-3)\sqrt{3}} = \frac{1}{2n-1}. \tag{3}$$

If there are n intersections to an edge, there are $n-1$ of these distances, so the total distance is $\frac{n-1}{2n-1}$, which is less than $1/2$, as desired.

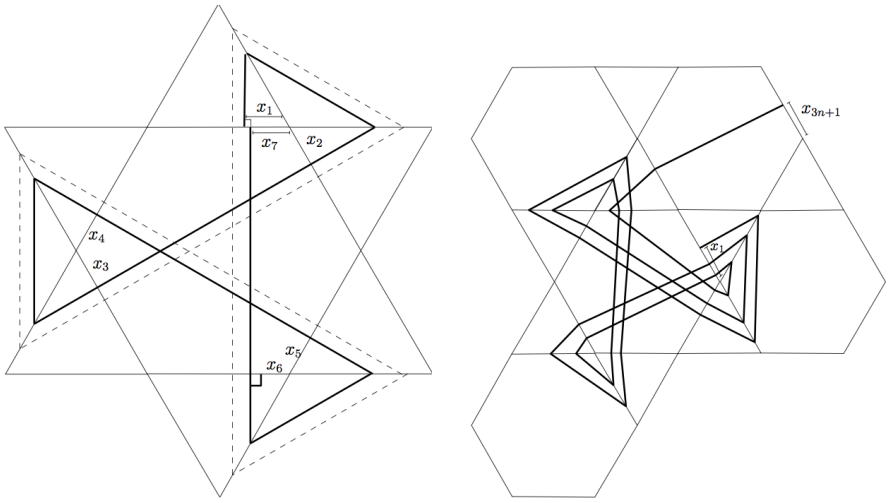

Figure 20: (a) The period-12 trajectory of Example 4.9, with lengths labeled for use in the proof of Proposition 4.10 (b) One period of the associated drift-periodic trajectory, where $n = 3$

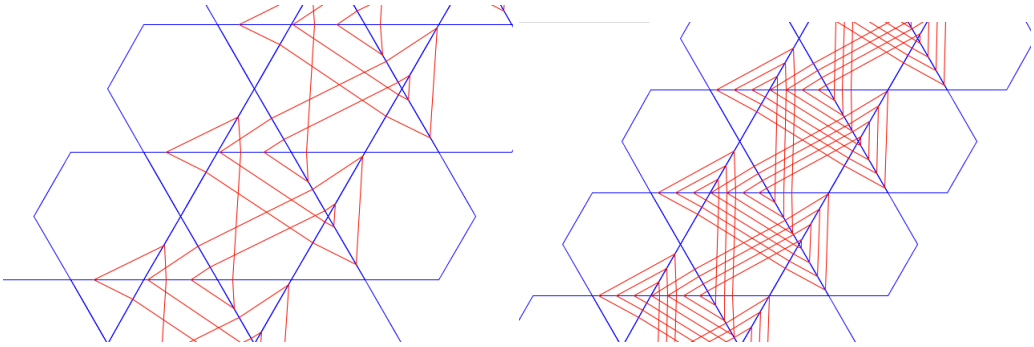

Figure 21: A drift-periodic trajectory with period (a) 18 and (b) 42, which are the $n = 2$ and $n = 4$ cases, respectively, of Proposition 4.10.

Now that we have the initial angle and initial starting point of the trajectory, we will show that the trajectory is drift-periodic, by showing that $x_1 = x_{12n-5}$ (Figure 20 (b)).

By the Trajectory Turner Lemma,

$$\alpha_{12k+4} = \pi - \alpha_{12k+1}, \quad \alpha_{12k+8} = \pi - \alpha_{12k+5}, \text{ and } \quad \alpha_{12k+12} = \pi - \alpha_{12k+9}.$$

By the Pentagon Lemma,

$$\alpha_{12k+5} = \pi - \alpha_{12k+4}, \quad \alpha_{12k+9} = \pi - \alpha_{12k+8}, \text{ and } \quad \alpha 12k + 13 = \pi - \alpha_{12k+12}.$$

Also, we know $\alpha_1 = \alpha$. Combining these yields

$$\alpha_{12k+1} = \alpha_{12k+5} = \alpha_{12k+9} = \alpha, \text{ and } \quad \alpha_{12k+4} = \alpha_{12k+8} = \alpha_{12k} = \pi - \alpha.$$

Also by the Trajectory Turner Lemma,

$$x_{12k+1} = x_{12k+4}, \quad x_{12k+5} = x_{12k+8}, \text{ and } \quad x_{12k+9} = x_{12k+12}$$

for all k.

By the Pentagon Lemma,

$$\begin{aligned}
x_{12k+5} &= x_{12k+4} + \sqrt{3}\cot(\pi - \alpha_{12k+4}) = x_{12k+4} + \sqrt{3}\cot(\alpha);\\
x_{12k+9} &= x_{12k+8} + \sqrt{3}\cot(\pi - \alpha_{12k+8}) = x_{12k+8} + \sqrt{3}\cot(\alpha);\\
x_{12k+13} &= x_{12k+12} + \sqrt{3}\cot(\pi - \alpha_{12k+12}) = x_{12k+12} + \sqrt{3}\cot(\alpha).
\end{aligned}$$

Combining these yields $x_{12k+13} = x_{12k+1} + 3\sqrt{3}\cot\alpha$, so the distance between p_{12k+13} and p_{12k+1} is $3\sqrt{3}\cot\alpha$. There are $n-1$ of these gaps, so $x_{12n-11} = x_1 + (n-1)3\sqrt{3}\cot\alpha$.

Now we apply the Trajectory Turner Lemma one more time:

$$x_{12n-8} = x_{12n-11}, \text{ and } \alpha_{12n-8} = \pi - \alpha_{12n-11}.$$

Now we apply the Quadrilateral Triangle Lemma and substitute in the relations from above:

$$\begin{aligned}
x_{12n-6} &= x_{12n-8} + \frac{1}{2} + \frac{\sqrt{3}}{2}\cot(\pi - \alpha_{12n-8})\\
&= x_{12n-11} + \frac{1}{2} + \frac{\sqrt{3}}{2}\cot(\alpha_{12n-11})\\
&= x_1 + (n-1)3\sqrt{3}\cot\alpha + \frac{1}{2} + \frac{\sqrt{3}}{2}\cot\alpha.
\end{aligned}$$

Finally, we apply the Pentagon Lemma and then substitute in the relations from above:

$$\begin{aligned}
x_{12n-5} &= x_{12n-6} + \sqrt{3}\cot(\pi - \alpha_{12n-6})\\
&= x_{12n-6} + \sqrt{3}\cot\alpha\\
&= x_1 + (n-1)3\sqrt{3}\cot\alpha + \frac{1}{2} + \frac{\sqrt{3}}{2}\cot\alpha + \sqrt{3}\cot\alpha\\
&= x_1 + \frac{1}{2} + \sqrt{3}\left(3n - 3 + 1 - \frac{1}{2}\right)\cot\alpha\\
&= x_1 + \frac{1}{2} + \frac{\sqrt{3}\,(3n - 3 + 1 - 1/2)}{-\sqrt{3}(6n-3)} = x_1 + \frac{1}{2} - \frac{1}{2} = x_1,
\end{aligned}$$

as desired.

□

Corollary 4.11. *By (3), the intersections to a selected edge are a distance $\frac{1}{2n-1}$ apart, so the limiting trajectory is dense in that edge, and thus dense on the neighboring tiles.*

Figure 21 shows two examples of the family of trajectories in Proposition 4.10; one can extrapolate what the limiting trajectory would look like. For some hexagons in the tiling, this limiting trajectory fills one part densely and does not visit another part of the hexagon at all. This is analogous to a billiard table in which a trajectory fills some region of the table densely and does not visit another part of the table at all [8].

Remark 4.12. As suggested by Figure 21, the drift-periodic trajectories of Proposition 4.10 converge to the period-12 trajectory of Example 4.9 as $n \to \infty$.

Also see the related periodic trajectories in Figure 22. Considering that the period-12 trajectory in Figure 20 yields the nearby drift-periodic trajectories in Figure 21, it is possible that a perturbation of these larger trajectories in will yield nearby drift-periodic trajectories.

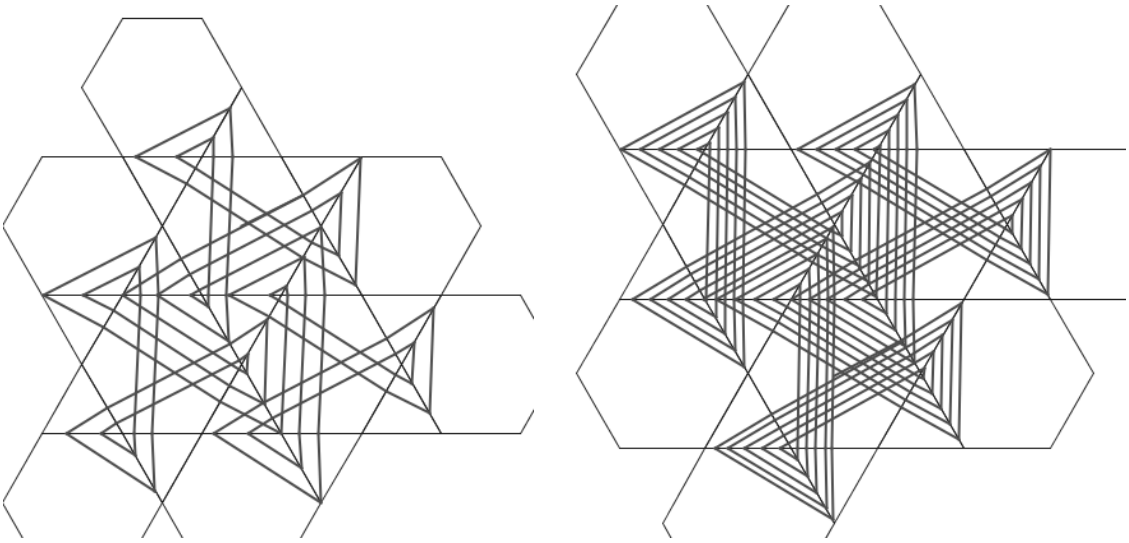

Figure 22: Trajectories with periods of 78 and 174

Example 4.13. There is a trajectory of period 24, with an initial angle of $\alpha = \pi - \tan^{-1}(2\sqrt{3})$.

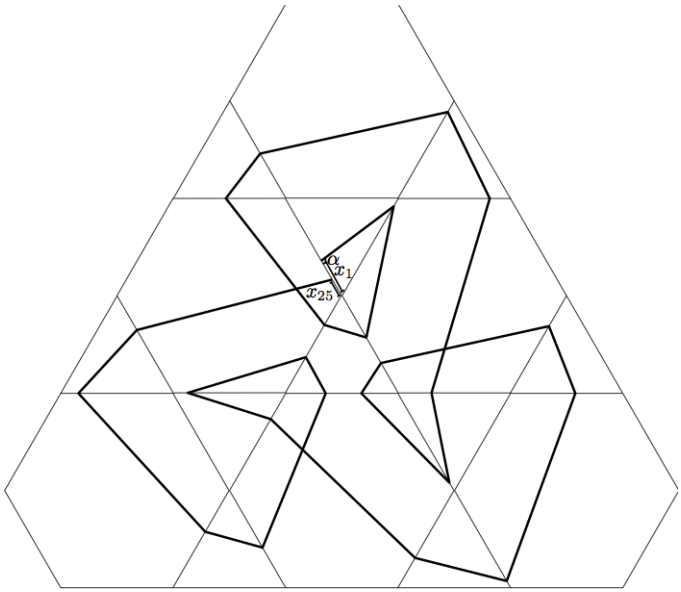

Figure 23: The trajectory of period 24 in Example 4.13

Proof. Define x_1 and x_{25} as in Figure 23.

By the Trajectory Turner Lemma, $x_{i+3} = x_i$ for $i = 1, 9, 17$. This does not change the value of the distance x_i.

By the Quadrilateral Triangle Lemma, $x_{i+2} = x_i + \frac{1}{2} + \frac{\sqrt{3}}{2}\cot\alpha$ for $i = 4, 6, 12, 14, 20, 22$. This results in adding $\frac{1}{2} + \frac{\sqrt{3}}{2}\cot\alpha$ to the distance x_i a total of 6 times, for a total increase of $3+3\sqrt{3}\cot\alpha$.

By the Pentagon Lemma, $x_{i+1} = x_i + \sqrt{3}\cot\alpha$ for $i = 8, 16, 24$. This results in adding $\sqrt{3}\cot\alpha$ to the distance x_i a total of 3 times, for a total increase of $3\sqrt{3}\cot\alpha$.

Thus $x_{25} = x_1 + 3 + 6\sqrt{3}\alpha$. The substitution $\cot\alpha = \frac{-1}{2\sqrt{3}}$ yields $x_{25} = x_1$, as desired.

□

Remark 4.14. Also see the larger periodic trajectories in Figure 24 that resemble the trajectory in Figure 23.

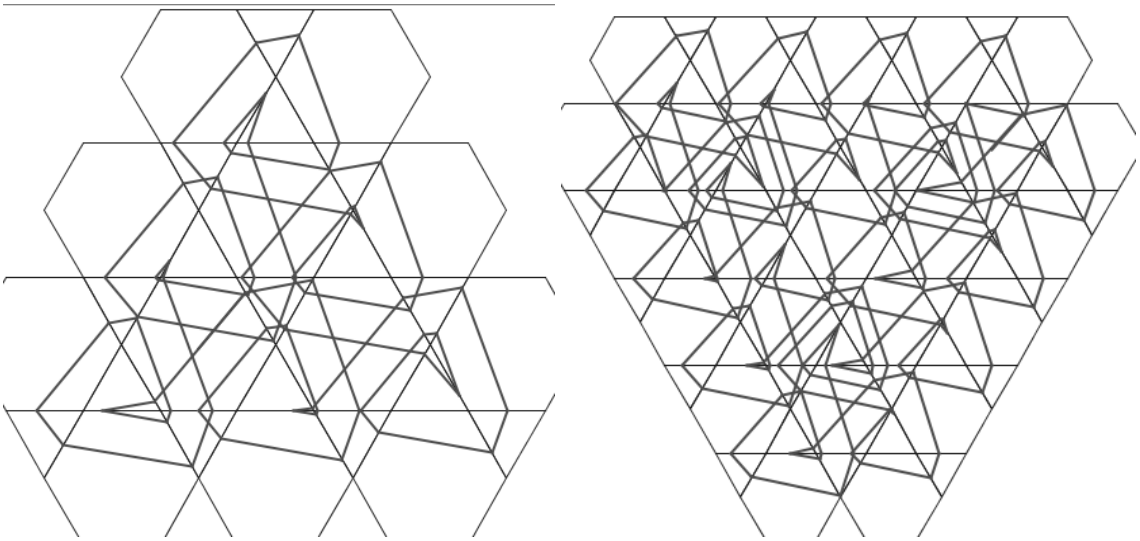

Figure 24: Trajectories with periods of 66 and 192

5 Future directions

Divisions of the plane: In this paper, we only studied divisions of the plane by finitely many non-parallel lines. One could relax these conditions, and study divisions of the plane with infinitely many lines, or include parallel lines. The unique feature of a division of the plane by lines is that there are regions of infinite area; one could study other tilings that have this property, such as a division of the plane by the curves $y = \sin(x) + k$ for $k \in \mathbf{Z}$, or related piecewise-linear curves.

Triangle tilings: We have many conjectures about triangle tilings based on experimental results; these are described in Section 3. We already showed that all triangle tilings have a trajectory of period 6 (Corollary 3.2) and that nearly all have a trajectory of period 10 (Theorem 3.11). Conjecture 3.13 says that all periodic trajectories on triangle tilings are of the form $4n + 2$; we would like to know, for a given n, which triangle tilings have a trajectory of period $4n + 2$.

Our results on these triangle tilings are elegant in the cases where the system is very stable. In contrast, the trihexagonal system is very unstable. We would like to understand what feature of a tiling causes this stability or instability. The triangle and trihexagonal tilings both have half-turn symmetry at each vertex, and in both cases the lines of the tiling are *not* lines of reflective symmetry for the tiling, so this is not the explanation. In tilings of triangles where some lines *are* lines of reflective symmetry for the tiling, such as isosceles triangle tilings and the tilings in Figure 2, the behavior of trajectories is very predictable.

Because the congruent triangle tilings we consider are those created by adding parallel diagonals to a parallelogram tiling, a next step would be to investigate this system on the parallelogram tiling itself. Another possibility is to consider edge-to-edge triangle tilings meeting 6 to a vertex, where the orientation of every other row of triangles is opposite. Still another direction is to consider tilings of congruent triangles that are not edge-to-edge; the congruent triangle tilings that we consider are a two-parameter family, and allowing this offset adds an additional parameter. Each of these tilings is pictured in Figure 25.

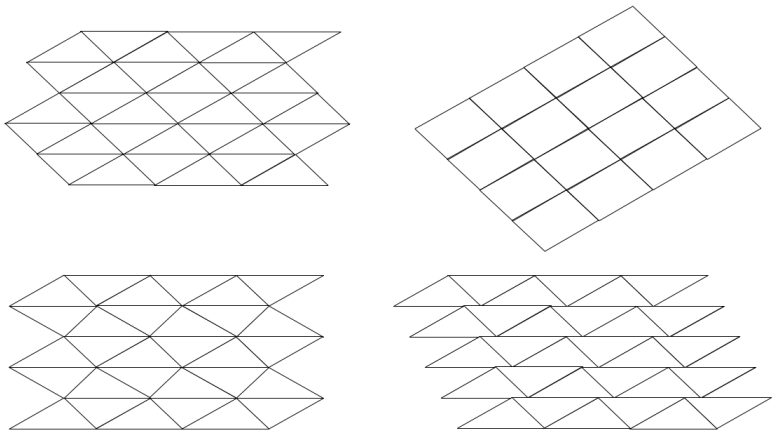

Figure 25: A triangle tiling of the kind we study, and three related tilings

The trihexagonal tiling: This tiling exhibits a surprising level of instability. We were unable to find a single stable trajectory in the tiling; during experimentation, even a tiny change in the direction or starting location of a trajectory would produce wildly different behavior. This is in marked contrast to some triangle tilings, where even a large change in direction or starting location had almost no effect on the behavior. We would like to understand why the trihexagonal tiling is so unstable. Examples of periodic trajectories that we have found are in Figures 22-24, and we conjecture that there are periodic trajectories of arbitrarily high period.

Further extensions: Our work considered only highly regular tilings of the plane. It would be interesting to consider some more complex tilings, such as the Penrose tiling or random tilings.

Our work also considered only polygonal tilings; perhaps tilings or divisions of the plane by curves would yield interesting dynamics. Inner billiards on curved tables, such as ellipses, yields beautiful mathematics [14], and outer billiards on piecewise-circular curves were studied during our research program [17], so tiling billiards with curves are another possible direction.

Additionally, since the motivation for our work is refraction of light through solids, an obvious next step would be to study this problem in three dimensions, since any real-world application to creating perfect lenses or invisibility shields would likely require solid materials.

References

[1] W. Barker, R. Howe, *Continuous symmetry: from Euclid to Klein*, American Mathematical Society (2007).

[2] D. Dolgopyat, B. Fayad, *Unbounded orbits for semicircular outer billiards*, Annales Henri Poincaré, 10 (2009) 357-375.

[3] K. Engelman, A. Kimball: *Negative Snell's propagation*, 2012 (unpublished).

[4] P. Glendinning, *Geometry of refractions and reflections through a biperiodic medium* (unpublished).

[5] A. Kwan, J. Dudley, E. Lantz, *Who really discovered Snell's law?*, Physics World, p. 62, April 2002.

[6] A. Mascarenhas, B. Fluegel: *Antisymmetry and the breakdown of Bloch's theorem for light*, preprint.

[7] H. Masur, Closed trajectories for quadratic differentials with an application to billiards. Duke Mathematics Journal 53 (1986), no. 2, 307–314.

[8] C. McMullen, "Trapped," `http://www.math.harvard.edu/~ctm/gallery/billiards/trapped.gif`, accessed 9 June 2015.

[9] R. Schwartz, *Obtuse Triangular Billiards II: 100 Degrees Worth of Periodic Trajectories*, Experimental Mathematics, 18 (2008), No. 2, 137-171.

[10] R. Schwartz, *Outer billiards on kites*, Annals of Mathematics Studies 171. Princeton University Press (2009).

[11] R. Schwartz, *Outer billiards on the Penrose kite: Compactification and Renormalization*, Journal of Modern Dynamics, 2012.

[12] D. Smith, J. Pendry, M Wiltshire: *Metamaterials and negative refractive index*, Science, Vol. 305, pp. 788-792, 2004.

[13] R. A. Shelby, D. R. Smith, S. Schultz, *Experimental Verification of a Negative Index of Refraction*, Science, Vol. 292 no. 5514 pp. 77-79, 2001.

[14] Sergei Tabachnikov, *Geometry and Billiards*, Student Mathematical Library 30, American Mathematical Society, 2005.

[15] F. Vivaldi, A. Shaidenko, *Global stability of a class of discontinuous dual billiards*, Comm. Math. Phys. 110 (1987) 625-640.

[16] N. Wolchover: *Physicists close in on 'perfect' optical lens*. Quanta Magazine. 8 Aug 2013.

[17] Z. Yao, *Devil's Staircase – Rotation Number of Outer Billiard with Polygonal Invariant Curves*, arxiv: 1402.2319 (unpublished).

Diana Davis, Mathematics Department, Northwestern University, 2033 Sheridan Road, Evanston IL 60208, diana@math.northwestern.edu

Kelsey DiPietro, Department of Applied and Computational Mathematics and Statistics, University of Notre Dame, 153 Hurley Hall, Notre Dame, IN 46556 kdipiet1@nd.edu

Jenny Rustad, Department of Mathematics, University of Maryland, Mathematics Building, College Park, MD 20742, jrustad1@math.umd.edu

Alexander St Laurent, Department of Mathematics and Department of Computer Science, Brown University, 151 Thayer Street, Providence, RI 02912 alexander_st_laurent@brown.edu